Supplementary Information (SI) for Analytical Methods.
This journal is © The Royal Society of Chemistry 2025

Supplementary information

A portable optical device for quantitative detection of lithium in blood plasma

Zitong Ye[1], Ziwei Huang[1], Jie Zhou[1], Haonan Li[1], Muyang Zhang[1], Qinghao He[1], Hao Chen[1], Jiahua Zhong[1], Huiru Zhang[2], Zhuoting Han[3*], Lok Ting Chu[4*], Weijin Guo[1*]

[1*]Department of Biomedical Engineering, Shantou University, Shantou, 515063, Guangdong, China.
[2]Guangdong Foshan Lianchuang Graduate School of Engineering, Foshan, 528311, Guangdong, China.
[3*]Laboratory Medicine Department, The Second Affiliated Hospital of Guangdong Medical University, Zhanjiang, 515063, Guangdong, China.
[4*]Institute of Biochemistry and Molecular Biology, Guangdong Medical University, Zhanjiang, 524023, Guangdong, China.
[*]Corresponding authors. E-mails: 19775772@qq.com; ltchu@gdmu.edu.cn; guoweijin@stu.edu.cn.

Chemical Structure and Absorbance Characteristics of Porphyrinoid Reagent

In this study, the reagent used is chemically named 2,3,7,8,12,13,17,18-octabromo-5,10, 15,20-tetrakis(4-sulfonatophenyl)porphyrin, as shown in Formula I below [1]. Figure S1 shows the absorbance spectrum of the porphyrinoid reagent dissolved in water with sodium hydroxide [1]. Figure S2 presents the absorbance spectrum change after reaction between the porphyrinoid reagent and a serum sample containing 1 mmol/L Li^+, compared with a blank sample in which the serum was replaced by distilled water [1].

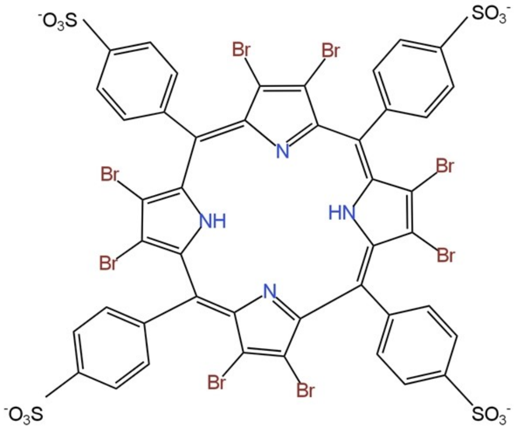

Formula I

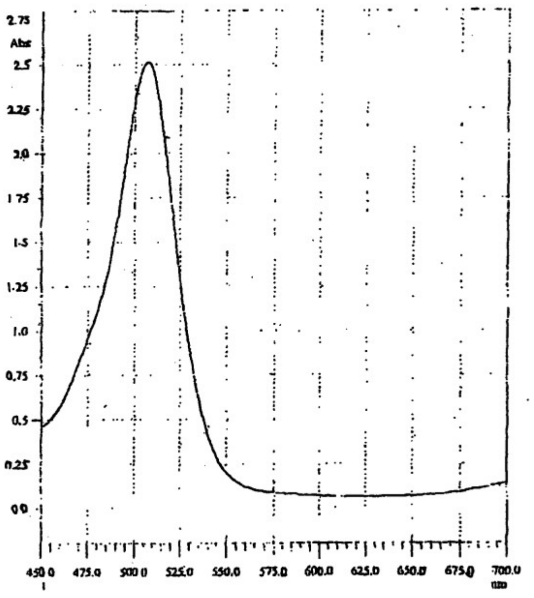

Figure S1. Absorbance spectrum of porphyrinoid reagent in aqueous alkaline solution [1].

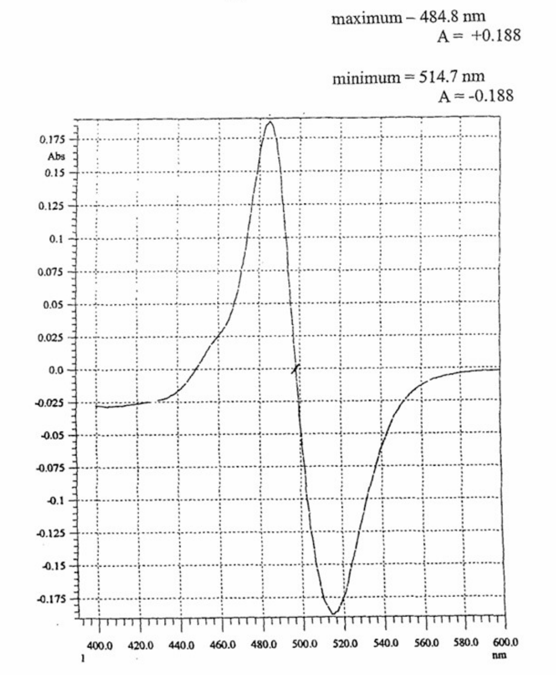

Figure S2. Absorbance spectrum of 1 mmol/L Li^+-spiked serum after reaction with porphyrinoid reagent, compared with blank [1].

Hardware Design and System Architecture

Figure S3(a) shows the circuit schematic of the portable Li^+ detection device. The system uses an STM32F407 microcontroller to control the light source, receive signals from the spectral sensor, and manage parameter setting and result display via a touchscreen. The user first calibrates the light intensity on the touchscreen. After passing through the sample, the light is detected by the spectral sensor and transmitted to the STM32F407, which calculates the absorbance difference and displays the corresponding Li$^+$ concentration. Figure S3(b) illustrates the software flow of the Li$^+$ detection device. After system initialization, the user sets parameters on Interface 1 to start detection. Once calibration is complete, the system enters Interface 2 for sequential data acquisition: blank, sample, and reacted values. The user can then choose to calculate and proceed to Interface 3 to view the results, with the option to return to Interface 2 to repeat the measurements. Figure S6 illustrates the circuit of the device along with the structure of its 3D-printed enclosure and labeled functional components.

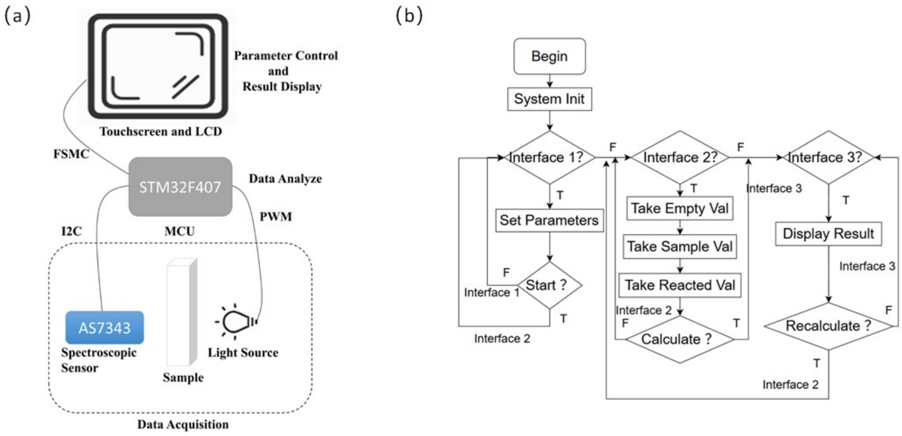

Figure S3. Circuit schematic of the device (a) and software flowchart (b).

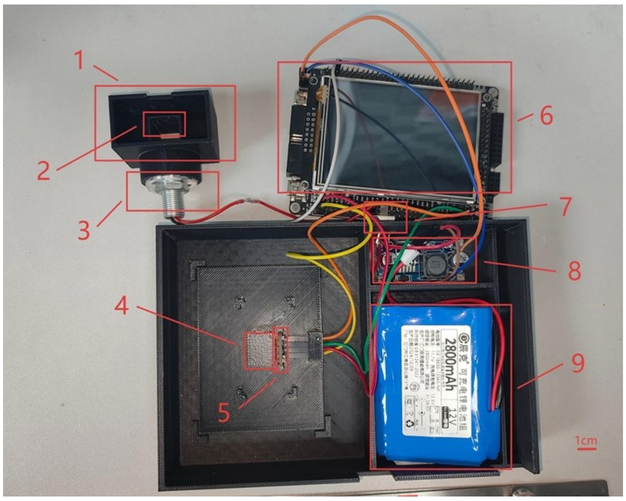

Figure S4. Photograph of the device circuit and 3D-printed enclosure structure. Labeled components: 1 – Detection chamber, 2 – Light shield, 3 – Light source, 4 – Base, 5 – Spectral sensor, 6 – Parameter control and display unit, 7 – Switch, 8 – Voltage stabilizer, 9 - Power supply module.

Detection Process

The procedure for detecting plasma lithium in practice is illustrated in Figure S5. First, after automatically calibrating the light intensity, place an empty cuvette into the cuvette holder and close the lid to measure the transmitted light intensity of the empty cuvette (n_0), as shown in Figure S5(a). Next, mix 3.0 μL of plasma with 240 μL of PBS, transfer 55 μL of the mixture into a plastic cuvette, place it into the holder, close the lid, and measure the transmitted light intensity (n_1), as shown in Figure S5(b). Then, add 25 μL of porphyrinoid reagent to the cuvette, vortex for 15 s, place the cuvette back into the holder, close the lid, and measure the transmitted light intensity (n_2), as shown in Figure S5(c). Using the formula $\Delta A = \lg\frac{n_0}{n_2} - \lg\frac{n_0}{n_1}$ to calculate the absorbance difference (ΔA), and compare it with the calibration curve to determine the plasma lithium concentration. During the detection, all transmitted light intensities are exclusively measured through the 505–520 nm wavelength channel.

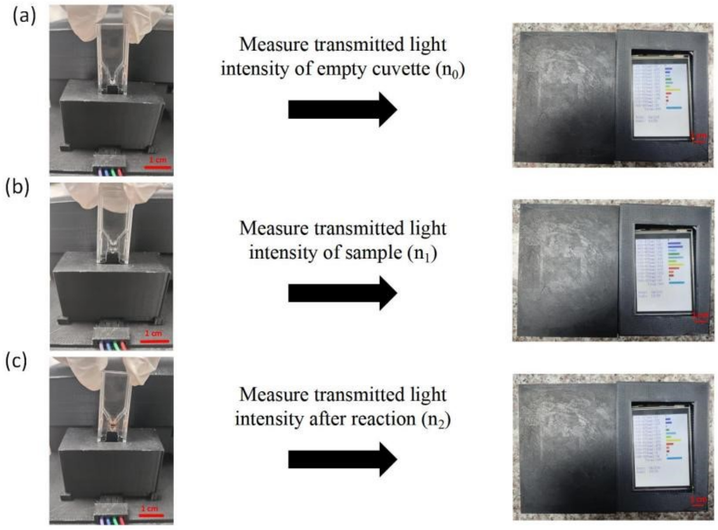

Figure S5. Detection process. Place the cuvette into the cuvette slot, close the lid, and then read the measurement value displayed on the interface.

User Interface and Operation

First, click button 1 on Interface 1 to calibrate the light intensity parameters and set it to 220. After the calibration is completed, click button 2 on Interface 1. The system will enter the Interface 2 and sequentially perform key data collection on Interface 2: button 3 measures the transmittance of the empty cuvette, button 4 measures the transmittance of the sample to be tested, and button 5 measures the transmittance after the porphyrinoid reagent reaction. After completing the data collection, click button 6 for calculation and proceed to Interface 3. Interface 3 will display the absorbance difference and the corresponding Li^+ concentration. At this point, the user can press button 7 to repeat the measurement.

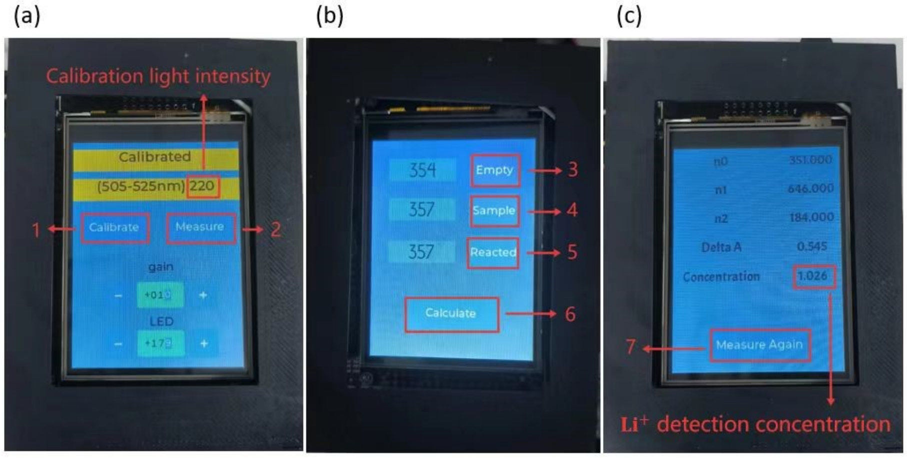

(505-525nm) 220

+01
+17

354
357
357

n0 351.000
n1 646.000
n2 184.000
Delta A 0.545
Concentration 1.026

Interface 1

Interface 2

Interface 3

Figure S6. Operation interface diagram of the device.

Evaluation of Within-Batch and Between-Batch Precision and Accuracy

To evaluate precision and accuracy, measurements were performed on plasma from the same individual spiked with the same lithium concentration (within-batch), and independent measurements were conducted on spiked plasma samples from different individuals (between-batch), each experiment was repeated for at least 6 times.

Table S1. Evaluation of within-batch and between-batch precision and accuracy of the portable lithium detection device

Analysis Type	Spiked Li^+ (mmol/L)	Measured Concentration (mmol/L)	RSD (%)	Recovery (%)
Within-Batch	1.4	1.41	3.5	100.4
Between-Batch	1.2	1.175	13.7	97.9

Ion Interference and Selectivity Evaluation

The experimental data demonstrate that the measurement of Li^+ concentration using this detection method is minimally affected by interference from other metal ions. This selectivity arises from the size-matching between the porphyrinoid cavity and Li^+ (radius 73 pm), while larger ions like Na^+ (113 pm) and K^+ (151 pm) fail to coordinate effectively. Given the high dilution factor of the samples and the extremely low concentration of transition metals in plasma, the impact of these metal ions on the detection results is considered negligible.

Table S2. Selectivity of Li^+ detection using our device

Interfering Ion	Spiked Li^+ Concentration (mmol/L)	Interfering Ion Concentration (mmol/L)	Li^+ Measured Concentration (mmol/L)	Recovery
-	1	-	1.06	106%

Na^+	1	140	1.07	107%
K^+	1	4	1.06	106%
Mg^{2+}	1	1	0.98	98%
Mn^{2+}	1	1	1.02	102%
Cr^{3+}	1	0.004	1.01	101%
Ca^{2+}	1	3	0.95	95%
Fe^{3+}	1	0.03	0.91	91%
Zn^{2+}	1	0.03	0.98	98%
Cu^{2+}	1	0.03	1.01	101%
Na^+, K^+	1	140 (Na^+), 4 (K^+)	1.07	107%

Cost Analysis of Detection Device and Per-Test

Table S3 and S4 present the cost of the detection device and the details of the expenses for each single test respectively. These tables contain detailed information of all components of the detection device as well as the raw materials and quantities required for each test.

Table S3. Cost estimation of the device

Materials	Cost per Device
STM32F407VET6 (Microcontroller)	7.03 USD
LED light	0.66 USD
PLA (for 3D printing)	1.3617 USD
Visible spectrum sensor (VS7343)	12.28 USD
3.2-inch touch screen	8.28 USD
DC-DC step-down module	0.41 USD
Toggle switch	0.06 USD
12 V lithium battery pack	4.66 USD
Total	34.7417 USD

Table S4. Cost estimation of single plasma lithium test

Materials	Unit cost	Materials per Device	Cost per Device
Cuvette	1.3448 USD/piece	1 piece	1.3448 USD
Porphyrinoid	0.0112 USD/μL	25 μL	0.28 USD
PBS	0.00000014 USD/μL	240 μL	0.0000336 USD
		Total	1.6248336 USD

Comparison of Analytical Performance Between Our Device and Reported Lithium Detection Methods

Table S5 summarizes the analytical performance of our lithium detection device in comparison with representative reported methods. Metrics include recovery rate, linear regression, relative standard deviation (RSD), detection time, and sample type. Linear regression evaluates accuracy by comparing detected and true values. As shown, our device performs comparably to or better than existing methods in major aspects, demonstrating high accuracy, fast response, and suitability for plasma-based point-of-care testing.

Table S5. Comparison of analytical performance between our device and reported lithium detection methods

Reference	Our Device	[2]	[3]	[4]	[5]
Recovery(%）	97.9	90-97.6	87-115	100.3±1.07	-
Linear Regression	$y = 1.03x - 0.095$	-	$y = 1.08x - 0.05$	-	$y = 0.96x + 0.03$
RSD (%)	8.7	3.4-9.8	-	-	7.1-13
Time	2 mins	10 s	40 s	<1 mins	3.5 mins
Sample	Plasma	Blood	Blood	Plasma	Capillary blood

References

[1] Balazs, N.D.H., Secombe, J.W.: Lithium detection in liquid biological samples and reagents therefor. US Patent 7241623 (2007)

[2] Komatsu, T., Maeki, M., Ishida, A., Tani, H., Tokeshi, M.: based device for the facile colorimetric determination of lithium ions in human whole blood. ACS sensors 5(5), 1287–1294 (2020)

[3] Novell, M., Guinovart, T., Blondeau, P., Rius, F.X., Andrade, F.J.: A paper-based potentiometric cell for decentralized monitoring of li levels in whole blood. Lab on a Chip 14(7), 1308–1314 (2014)

[4] Sweilam, M.N., Varcoe, J.R., Crean, C.: Fabrication and optimization of fiber-based lithium sensor: a step toward wearable sensors for lithium drug monitoring in interstitial fluid. ACS sensors 3(9), 1802–1810 (2018)

[5] Floris, A., Staal, S., Lenk, S., Staijen, E., Kohlheyer, D., Eijkel, J., Berg, A.: A prefilled, ready-to-use electrophoresis based lab-on-a-chip device for monitoring lithium in blood. Lab on a Chip 10(14), 1799–1806 (2010)